Luminescence of Eu^{3+} doped calcium hydroxyapatite and tricalcium phosphate powders

© I.D. Sidorov,[1] T.M. Minnebaev,[1] E.I. Oleynikova,[1] A.S. Nizamutdinov,[1] M.S. Pudovkin,[1] M.R. Gafurov,[1] Yu.O. Nikitina,[2] A.Yu. Demina,[2] N.V. Petrakova,[2] V.S. Komlev[2]

[1] Kazan Federal University, Institute of Physics,
420008 Kazan, Russia
[2] Baikov Institute of Metallurgy and Materials Science, Russian Academy of Sciences,
119334 Moscow, Russia
e-mail: Sidorov.I.D@mail.ru

The use of calcium phosphates as a basis for prosthetic materials for musculoskeletal injuries and luminescent probes is a promising direction because these compounds correspond to the mineral composition of bone. The results of a study of the spectral and luminescence decay of Eu^{3+} ions in hydroxyapatite and tricalcium phosphate matrices after synthesis and after heat treatment at 1573 K in air are discussed. A study of luminescence using a UV laser revealed lines characteristic of Eu^{3+} in both materials: the $^5D_0 \rightarrow {}^7F_0$ and $^5D_0 \rightarrow {}^7F_2$ transitions have the highest line intensity. Heat treatment led to a change in the spectral and kinetic characteristics: a significant effect on the shape of spectral lines and lifetimes was found. The luminescence decay of the samples at a wavelength of 622.7 nm before heat treatment is biexponential, which indicates the presence of nonequivalent positions of Eu^{3+} ions in the matrices. For a hydroxyapatite sample, annealing leads to the resolution of Stark components and intense luminescence at a wavelength of 573.7 nm, which indicates, the luminescence lifetime increases. For a tricalcium phosphate sample, annealing also leads to the resolution of Stark components in the luminescence spectrum, the luminescence decay becomes single-exponential with higher luminescence lifetime.

Keywords: hydroxyapatite, tricalcium phosphate, Eu^{3+} ion, luminescence, luminescence decay, nonequivalent positions of Eu^{3+}.

Introduction

Synthetic calcium phosphates, such as calcium hydroxyapatite (HA) $Ca_{10}(PO_4)_6(OH)_2$ and tricalcium phosphate (TCP) $Ca_3(PO_4)_2$, are a promising basis for subcutaneously or intravenously administered luminescent probes or prosthetics of musculoskeletal injuries. Such materials should not cause undesirable reactions with surrounding tissues and interstitial fluids, i.e. should have biological compatibility and biological activity. This is possible due to the correspondence of these substances to the mineral composition and the ratio of Ca/P ions in the bone [1–3]. In addition, nanometer-scale calcium phosphates can adsorb proteins and drugs on themselves and deliver them to human cells. The addition of rare-earth allows to create phosphors that are stable over time, which distinguishes them favorably from organic ones [4]. By doping HA and TCP with two rare-earth ions, for example Eu and Gd, it is possible to increase the quantum yield of luminescence, and also to create multimodal contrast agents based on them, which will allow combining the methods of fluorescence analysis, MRI and CT [5–7].

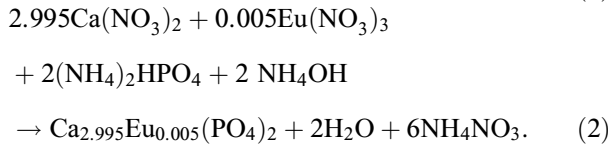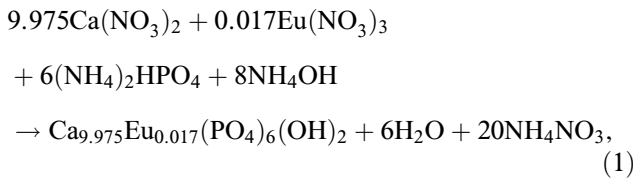In this work, we use HA and TCP samples synthesized by precipitation from aqueous solutions. The samples are doped with 0.25% molar Eu ions, which is approximately 0.25% by mass or 0.038% atomic.

The purpose of this work is to study the spectral and kinetic characteristics of the Eu^{3+} ion in HA and TCP matrices and the effect of annealing on them.

1. Materials and methods

Powders of Eu-containing calcium phosphates (PC-Eu) were obtained by precipitation from aqueous solutions. In this work, the following reagents from NPP „PanEko" (Moscow, Russia) were used: calcium nitrate $Ca(NO_3)_2 \cdot 4H_2O$ of chemically pure grade, ammonium hydrogen phosphate $(NH_4)_2HPO_4$ of analytic grade, 25% aqueous ammonia solution NH_4OH of analytic grade, $Eu(NO_3)_3 \cdot 6H_2O$ of chemically pure grade, distilled water in accordance with GOST 6709-72. The amount of Eu was calculated relative to the atomic content of Ca in HA or TCP. A solution of Eu (III) nitrate with a concentration of 0.1 mol/l was added to a 0.5 mol/l solution of calcium nitrate, and a 0.5 mol/l solution of ammonium hydrogen phosphate was added dropwise to the resulting mixture; the pH environment was maintained at the level of 11.5 ± 0.5 for HA and 7.0 ± 0.5 for TCP by adding a 0.25% ammonia

solution. The amount of reactants was calculated according to reaction equations (1) for HA and (2) for TCP.

$$9.975Ca(NO_3)_2 + 0.017Eu(NO_3)_3$$

$$+ 6(NH_4)_2HPO_4 + 8NH_4OH$$

$$\rightarrow Ca_{9.975}Eu_{0.017}(PO_4)_6(OH)_2 + 6H_2O + 20NH_4NO_3, \quad (1)$$

$$2.995Ca(NO_3)_2 + 0.005Eu(NO_3)_3$$

$$+ 2(NH_4)_2HPO_4 + 2\ NH_4OH$$

$$\rightarrow Ca_{2.995}Eu_{0.005}(PO_4)_2 + 2H_2O + 6NH_4NO_3. \quad (2)$$

The materials are presented in two forms: HA and TCP powders with Eu after synthesis, HA and TCP powders with Eu after heat treatment at 1573 K in air. The particle size after synthesis is $10-20$ nm for HA and $100-150$ nm for TCP, the oxidation state of Eu is presumably 3+. The particle size of both powders after heat treatment is $0.5-1.0\,\mu$m, the oxidation state of Eu may have changed.

The specific surface area (SSPEC) of the experimental powders was measured using the Brunauer–Emmett–Teller (BET) low-temperature nitrogen adsorption method on a Tristar 3000 analyzer (Micromeritics, USA). Using the obtained BET data, the average particle diameter was calculated in the approximation of a spherical shape and equal particle diameter (D_{BET}) in accordance with the formula

$$D_{BET} = \frac{6000}{S_{SPEC} \cdot \rho}, \quad (3)$$

where ρ — theoretical density (3.156 g/cm^3 for HA, 3.067 g/cm^3 for TCP). Diffraction patterns were recorded using a D2 Phaser diffractometer (Bruker, USA), operating in Bragg–Brentano geometry with CuKa radiation ($\lambda = 1.5418$ Å), range 2θ from $10°$ to $70°$, step size $0.02°$, with a speed of 1.0 s/step. The phases were determined using the JCPDS-PDF2 database.

Luminescence was excited using a LOTIS TII LS-2147 UV laser with a wavelength $\lambda = 266$ nm. With the help of lenses, the excitation was focused into a spot with a diameter of 2 mm and aimed at the object of study. Luminescence radiation was fed through a waveguide to the Aurora4000 spectrometer. To measure the kinetic properties, an MDR-23 monochromator was used with a FEU-100 photoelectric multiplier, which was connected to a Tektronix DPO 7254C oscilloscope.

Figure 1 shows X-ray diffraction analysis (XDA) of experimental powders. In the diffraction pattern of the HA powder after synthesis, a set of broadened low-intensity X-ray peaks was assigned to a set of HA peaks (card from the JCPDS-PDF2 database № 09-0342) (Fig. 1, *a*). This is due to the formation of a highly dispersed sediment with a low degree of crystallinity (amorphous state), which is explained by deposition at room temperature. This result is consistent with the literature data [8,9]. The diffraction pattern of the heat-treated HA powder consisted of a set of narrow, high-intensity peaks that fully corresponded to the HA phase
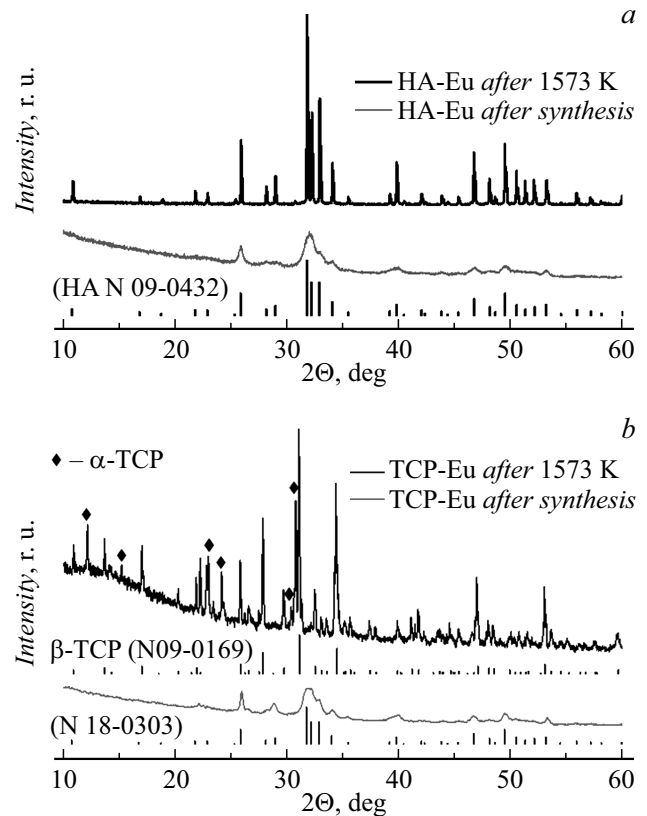

Figure 1. *a* — X-ray diffraction patterns of HA with Eu^{3+} after synthesis and after heat treatment at 1573 K; *b* — X-ray diffraction patterns of TCP with Eu^{3+} after synthesis and after heat treatment at 1573 K.

(card № 09-0432) with a high degree of crystallinity. The particle size for powders given above according to BET data (nano- and micro-scale, respectively, for HA after synthesis and heat treatment) confirms these results.

Figure 1, *b* shows diffraction patterns for TCP powders after synthesis and heat treatment. After synthesis, the powder was classified as amorphous calcium phosphate with a low degree of crystallinity ($Ca_3(PO_4)_2 \cdot nH_2O$, card from the JCPDS-PDF2 database № 018-0303), which is typical for the synthesis conditions used: level pH = 7, temperature $293-297$ K, filtering from stock solution without aging [9,10]. When analyzing the diffraction pattern of heat-treated TCP, it should be noted that after heating, TCP exists in two modifications: the orthorhombic β phase and the monoclinic α phase (two more modifications exist at temperatures above 1573 K and high pressures). The low-temperature β modification of TCP without impurities is stable up to 1393 K; over this temperature, a phase transformation occurs into the monoclinic α modification. The presence of cation substitutions in the TCP structure leads to a shift in the phase transition temperature. Thus, the content of Mg, Sr, Zn, Ce leads to stabilization of the β phase over the phase transition temperature [11–13]. In this regard, as a result of the introduction of the Eu dopant into the structure of TCP during deposition and

heat treatment at a temperature significantly higher than the phase transformation temperature (1573 K), the presence of the low-temperature β modification of TCP in the composition of the low-temperature modification indirectly judged the successful cationic substitution of Ca^{2+} ions to Eu^{3+} ions. Returning to the XDA data, the heat-treated sample revealed the presence of a mixture of modifications α-TCP and β-TCP, which indicates the incorporation of Eu ions into the TCP structure through cationic substitution.

2. Results and discussion

In the luminescence spectrum of HA with Eu^{3+}, presented in Fig. 2, the highest luminescence intensity is observed for the transitions $^5D_0 \rightarrow {}^7F_0$ (573.7 nm) and $^5D_0 \rightarrow {}^7F_2$ (600−640 nm). A distinctive feature of HA is the presence of two positions of Ca^{2+} ions, which are substituted by Eu^{3+} ions. The position I of Ca^{2+}ion has high symmetry C_3 and is surrounded by 9 oxygen ions. The position II of Ca^{2+} ion has low symmetry C_S, surrounded by 6 oxygen atoms and 1 ion $(OH)^-$. Due to the substitution of the Ca^{2+} ion in position II by the Eu^{3+} ion, the transition $^5D_0 \rightarrow {}^7F_0$ [14–17] is allowed. The luminescence intensity of the sample before treatment is relatively low. Heat treatment leads to significant changes in the width and from of the spectral lines; the luminescence intensity increases, namely, the Eu^{3+} lines characteristic of HA as a matrix with well-resolved Stark components appear. This may indicate a change in the phase of the sample. This result is consistent with the results of X-ray diffractometry.

Figure 3 shows the luminescence spectrum of TCP powders before and after heat treatment. After heat treatment of TCP with Eu^{3+}, the luminescence intensity also increases, and spectrally resolved lines of Stark components appear. The main contribution to the luminescence of TCP with Eu^{3+} comes from the transition $^5D_0 \rightarrow {}^7F_2$ (600−640 nm).
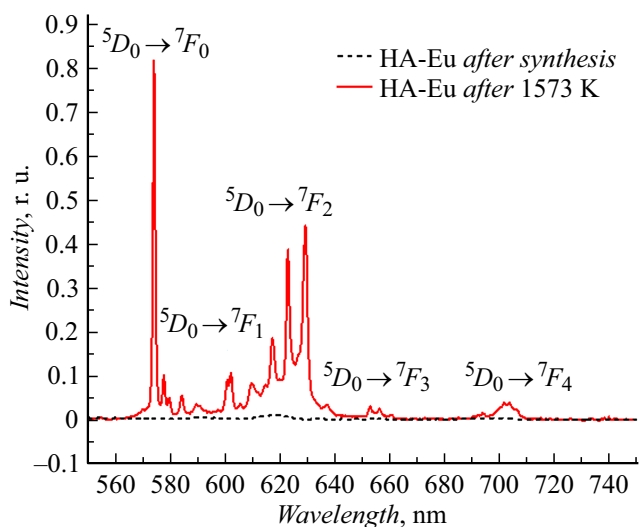
Figure 2. Luminescence spectrum of HA with Eu^{3+} before and after heat treatment.
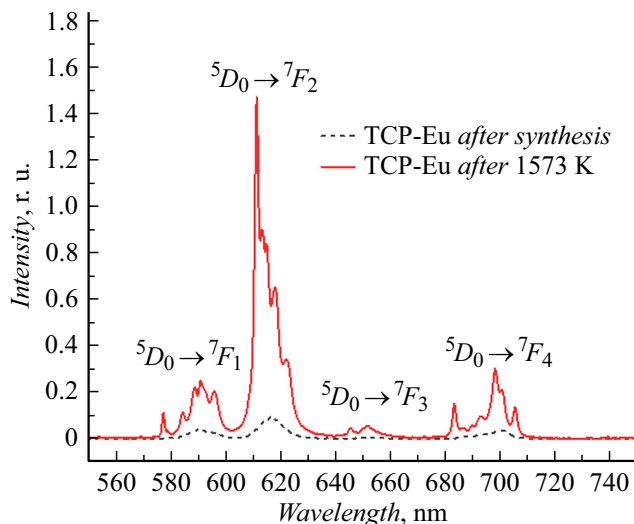
Figure 3. Luminescence spectrum of TCP with Eu^{3+} before and after heat treatment.

To gain a deeper understanding of changes in materials during additional heat treatment, the decay of Eu^{3+} luminescence at a wavelength of 622.7 nm was studied. The choice of this luminescence wavelength is due to the possibility of comparing the luminescence decay of the Eu^{3+} ion in the HA and TCP matrices with each other, since there is data on the possible transformation of the HA matrix into TCP [18]. Before treatment at a temperature of 1573 K, the HA sample has biexponential luminescence decay at a wavelength of 622.7 nm with times $263\,\mu s$ and 1.14 ms (Fig. 4,a), which can be attributed to the presence of two types of Eu^{3+} ion centers. The weight contributions of the short and long components are 0.899 and 0.101, respectively. After additional heat treatment, the luminescence decay remains biexponential; the luminescence lifetimes increased to the values $558\,\mu s$ and 1.47 ms with weighting coefficients of 0.977 and 0.023. It can be noted that after annealing, the relative contribution of the shorter component is predominant, which can be an evidence of the formation of a crystalline phase of hydroxyapatite.

For TCP samples the picture is less complex. As can be seen from Fig. 4,b, the luminescence decay of a sample of TCP powders before treatment at a wavelength of 622.7 nm is bi-exponential with times $164\,\mu s$ and 1.10 ms, weighting coefficients of 0.792 and 0.208, respectively. Benhamou and colleagues studied the positions of substitution of Ca^{2+} ions by Eu^{3+} ions in TCP [19]. They showed that Eu^{3+} ions are characterized by the substitution of Ca^{2+} in three nonequivalent positions M1, M2 and M3. Most of the Eu^{3+} is located at positions M1 and M2. This is explained by the fact that positions M1 and M2 are similar to each other in terms of a set of characteristics (number of neighbors, bond length, relative luminescence line intensity luminescence decay), while position M3 differs from them in a larger number of neighbors and, as a
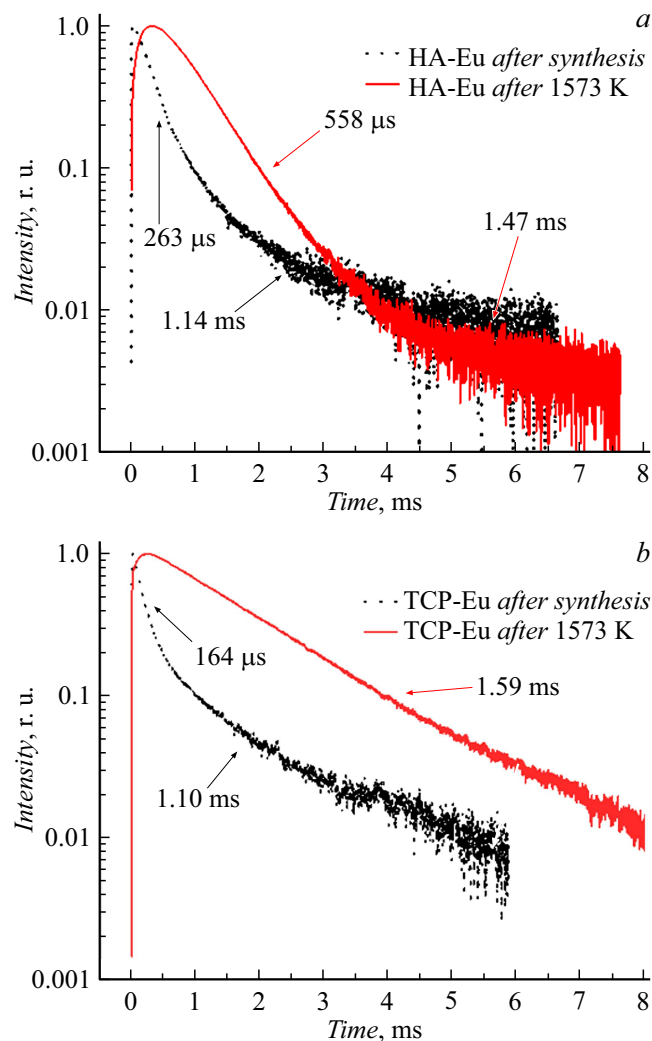
Figure 4. *a* — luminescence decay of HA powders with Eu^{3+} at a wavelength of 622.7 nm before and after heat treatment; *b* — luminescence decay of TCP powders with Eu^{3+} at a wavelength of 622.7 nm before and after heat treatment.

consequence, a larger length communications $Eu-O$ bond length. Increasing the bond length leads to an increase in the crystal field strength and a shortening of the luminescence lifetime. The uniqueness of the study is that the spectral and kinetic characteristics of luminescence were studied together with the structural study of the samples. Thus, we see biexponential luminescence decay due to the merging of contributions from positions M1 and M2 into one component. After heat treatment, the luminescence decay of the sample at a wavelength of 622.7 nm becomes single-exponential, and the lifetime takes on a value of 1.59 ms. It is assumed that the M3 position has a high probability of undergoing a phase transition due to the high crystal field strength, at the same time migration of Eu^{3+} ions to the M1 and M2 positions may occur. This corresponds to the transition of the sample into the crystalline TCP phase observed in X-ray diffraction patterns and luminescence spectra.

Conclusion

Thus, in our work we investigated the spectral and kinetic characteristics of luminescence of HA and TCP samples doped with Eu^{3+} ions before and after heat treatment at a temperature of 1573 K in conjunction with structural studies, which is new. It has been shown that thermal treatment of HA samples with Eu^{3+} and TCP with Eu^{3+} leads to an increase in the relative luminescence intensity and an increase in the luminescence lifetime. This may indicate a change in the phase composition as a result of heat treatment and is consistent with the results of X-ray diffraction analysis. However, a comparison of the luminescence decay characteristics of Eu^{3+} ions in these matrices for the transition $^5D_0 \rightarrow {}^7F_2$ revealed different patterns of changes as a result of additional thermal treatment for these matrices.

Funding

Conflict of interest

The authors declare that they have no conflict of interest.

References

[1] Yu.O. Nikitina. Avtoref. kand. diss. (IMET RAS, M., 2022) (in Russian)

[2] A.M. Nikolaev, I.E. Kolesnikov, O.V. Frank-Kamenskaya, M.A. Kuzmina. Pat. RU № 2628610, Rossiyskaya Federatsiya, MPK C09K11/71. *Sposob polucheniya nanorazmernogo vysokolyuminestsentnogo apatita s primes'yu yevropiya (Eu)* (№ 124206; zayavl. 17.06.2016; opubl. 21.08.2017) (in Russian).

[3] Yu.O. Nikitina, N.V. Petrakova, S.A. Kozyukhin, V.S. Komlev, S.M. Barinov. Pat. RU № 2779453, Rossiyskaya Federatsiya, MPK C01B25/32. *Sposob polucheniya lyuminestsentnogo ortofosfata kal'tsiya, aktivirovannogo tseriyem* (№ 136552; zayavl. 10.12.2021; opubl. 07.09.2022) (in Russian).

[4] A. Doat, M. Fanjul, F. Pellé, E. Hollande, A. Lebugle. Biomaterials, **24** (19), 3365 (2003). DOI: 10.1016/S0142-9612(03)00169-8

[5] A. Ashokan, D. Menon, S. Nair, M. Koyakutty. Biomaterials, **31** (9), 2606 (2010). DOI: 10.1016/j.biomaterials.2009.11.113

[6] S. Mondal, V.T. Nguyen, S. Park, J. Choi, T.M.T. Vo, J.H. Shin, Y.H. Kang, J. Oh. Ceram. Intern., **46** (18), 29249 (2020). DOI: 10.1016/j.ceramint.2020.08.099

[7] A. Tesch, C. Wenisch, K.H. Herrmann, J.R. Reichenbach, P. Warncke, D. Fischer, F.A. Müller. Mater. Sci. Eng., **81**, 422 (2017). DOI: 10.1016/j.msec.2017.08.032

[8] S.V. Dorozhkin. Intern. J. Mater. Chem., **2** (1), 19 (2012). DOI: 10.5923/j.ijmc.20120201.04

[9] I.E. Glazov, V.K. Krut'ko, O.N. Musskaya, A.I. Kulak. Russ. J. Inorg. Chem., **67**, 173 (2022). DOI: 10.1134/S0036023622020048

[10] M. Bohner, B.L.G. Santoni, N. Döbelin. Acta Biomaterialia, **113**, 23 (2020). DOI: 10.1016/j.actbio.2020.06.022

[11] L. Sinusaite, A. Kareiva, A. Zarkov. Crystal Growth & Design, **21** (2), 1242 (2021). DOI: 10.1021/acs.cgd.0c01534

[12] R. Enderle, F. Götz-Neunhoeffer, M. Göbbels, F.A. Müller, P. Greil. Biomaterials, **26** (17), 3379 (2005). DOI: 10.1016/j.biomaterials.2004.09.017

[13] Yu.O. Nikitina, N.V. Petrakova, S.A. Kozyukhin, V.P. Sirotinkin, A.A. Konovalov, Yu.F. Kargin, S.M. Barinov, V.S. Komleva. Inorg. Mater., **59** (4), 394 (2023). DOI: 10.1134/S002016852304009X

[14] O.A. Graeve, R. Kanakala, A. Madadi, B.C. Williams, K.C. Glass. Biomaterials, **31** (15), 4259 (2010). DOI: j.biomaterials.2010.02.009

[15] E.V. Zubar. Nanosistemi, nanomateriali, nanotekhnologiï, **7** (2), 581 (2009) (in Russian).

[16] N.I. Steblevskaya, M.V. Belobeletskaya, A.Yu. Ustinov, M.A. Medkov. Zhurn. neorgan. khimii, **64** (2), 146 (2019) (in Russian). DOI: 10.1134/S0044457X19020211

[17] E.J. Kim, S.W. Choi, S.H. Hong. J. American Ceram. Society, **90** (9), 2795 (2007). DOI: 10.1111/j.1551-2916.2007.01791.x

[18] M. Macintosh, Q. Yao, J. Xu, Z. Dong, L.Y. Chang, L. Liu. Ceram. Intern., **47** (8), 11387 (2021). DOI: 10.1016/j.ceramint.2020.12.265

[19] R.A. Benhamou, A. Bessiere, G. Wallez, B. Viana, M. Elaatmani, M. Daoud, A. Zegzouti. J. Solid State Chem., **182** (8), 2319 (2009). DOI: 10.1016/j.jssc.2009.06.01

Translated by A.Akhtyamov